

FLUVIAL CHANNELS ON TITAN

by

Nicole Faith Baugh

A Thesis Submitted to the Faculty of the
DEPARTMENT OF PLANETARY SCIENCES
In Partial Fulfillment of the Requirements
For the Degree of
MASTER OF SCIENCE
In the Graduate College
THE UNIVERSITY OF ARIZONA

2008

STATEMENT BY AUTHOR

This thesis has been submitted in partial fulfillment of requirements for an advanced degree at The University of Arizona and is deposited in the University Library to be made available to borrowers under rules of the Library.

Brief quotations from this thesis are allowable without special permission, provided that accurate acknowledgement of source is made. Requests for permission for extended quotation from or reproduction of this manuscript in whole or in part may be granted by the head of the major department or the Dean of the Graduate College when in his or her judgment the proposed use of the material is in the interests of scholarship. In all other instances, however, permission must be obtained from the author.

SIGNED: Nicole Faith Baugh

APPROVAL BY THESIS DIRECTOR

This thesis has been approved on the date shown below:

Robert H. Brown
Dr. Robert H. Brown
Professor of Planetary Sciences

4/22/2008
Date

ACKNOWLEDGEMENTS

Many people deserve acknowledgement for their assistance in my grad school career. First, to my advisor Robert Brown, many thanks for his support and advice (and the occasional kick in the seat of the pants). Second, I'd like to thank the many professors at LPL who shared their scientific expertise with me. To David Schleicher at Lowell Observatory, thanks for the chance to play with telescopes and for being a sounding board. Finally, I owe a huge debt of gratitude to my undergraduate physics professors at Furman and Augusta State Universities, without whom I would not made it to graduate school in the first place (I can say with confidence that this thesis is the fault of one Bill Baker—thanks).

Thanks also to my fellow graduate students, in particular my year-mates. Having good people with me in the grad school pressure cooker kept me going. To Mandy Proctor and Julia Greissl, thanks for the many dinners, movies, arguments and celebrations. To the Angels campaign, for the evenings spent crying with laughter. Thanks also to Dennis Conner, who listened to way more than his fair share of whining without ever calling me on it.

Finally, as always, to my family, for their constant love, support and unswerving belief in my abilities—my mother, on whom I can always depend on for an honest answer, my sister, for her ability to put things into perspective for me when I can't, my uncle, who gave me his battered copy of the CRC math tables, and my grandmother, who will be sorely missed.

DEDICATION

This thesis is dedicated to my mother, Rosemary Forrest, who taught me to always make good decisions.

TABLE OF CONTENTS

LIST OF FIGURES	6
LIST OF TABLES	7
ABSTRACT	8
CHAPTER 1: INTRODUCTION	9
CHAPTER 2: DATASET AND MEASUREMENTS	12
2.1 Cassini RADAR.....	12
2.2 The SAR images	13
2.3 Channel measurements.....	13
CHAPTER 3: CHANNEL DESCRIPTIONS	16
3.1 Channel networks.....	16
3.2 Channels associated with surface features	19
3.3 Other channels on Titan	22
CHAPTER 4: RESULTS AND DISCUSSION.....	25
4.1 Channel lengths.....	25
4.2 Geographic distribution of the channels.....	28
4.3 Sediment budget on Titan.....	31
4.4 Channel network integration	37
CHAPTER 5: CONCLUSION AND FURTHER QUESTIONS.....	39
APPENDIX A: TABLE OF CHANNEL LENGTHS	41
REFERENCES.....	43

LIST OF FIGURES

FIGURE 3.1, Channel Networks.....	17
FIGURE 3.2, Channels Near Ganesa Macula.....	20
FIGURE 3.3, Channels Near Menrva Crater	23
FIGURE 3.4, Possible Channel Near Ksa Crater.....	24
FIGURE 4.1, Edge of the Western Xanadu Network.....	36
FIGURE 4.2, Stream Order in the Western Xanadu Network	38

LIST OF TABLES

TABLE 4.1, Length of Streams on Titan.....	27
TABLE 4.2, Stream Order and Channel Lengths for Titan's Channel Networks	27

ABSTRACT

We present channel length and stream order for possible fluvial channels present in Cassini Synthetic Aperture Radar (SAR) data from Ta to T19. These features are present at most latitudes observed, with the bulk of the channels located in near-equatorial latitudes. Many of them are also organized into four branching channel networks, three of third order and one of fourth order, similar to river systems on Earth and Mars. These networks appear well integrated, with few streams that are not incorporated into the higher order branches. The median channel length for all channels on Titan is 29 km, with the longest channels all being incorporated into the channel networks. Estimates of channel width and depth of 1 km and 100m respectively result in a channel volume of 10^{12} m^3 which, when extrapolated to the entire surface of Titan results in 10^{13} m^3 of sediment.

CHAPTER 1

INTRODUCTION

The Cassini Titan Radar Mapper has obtained synthetic aperture radar images of the moon's surface since the first pass of Titan (Ta) in October 2004 (Elachi *et al.* 2005). In many of these images channel-like features, some of which have been attributed to fluvial erosion, have been observed. These features appear in disparate locations on Titan, appear both radar-bright and radar-dark, and display several distinct, familiar morphologies similar to those on Earth or Mars. Several researchers have reported on the channels seen by the Huygens probe (e.g. Tomasko *et al.* 2005, Perron *et al.* 2006, Soderblom *et al.* 2007b) and those seen by Cassini RADAR (e.g. Lopes *et al.* 2007, Elachi *et al.* 2006, Barnes *et al.* 2007c).

The first RADAR paper to report channels (Elachi *et al.* 2005) observed features in the T3 swath that they stated could be interpreted as either cryovolcanic outflow features or as fluid-carved channels, but there was little additional evidence to support one hypothesis over another. However, the appearance of branched channels in the T3 (Elachi *et al.* 2006) swath provided further support for the idea of rainfall-driven channel creation on Titan, despite the results from Lopes *et al.* (2007) that convincingly attribute many of the TA features to cryovolcanism. Data from the Huygens probe descent and post-landing images (Tomasko *et al.* 2005) showed what appeared to be an extensive network of channels leading to an apparent old coastline, with rounded cobbles providing

yet more proof of liquid methane pluvial processes. Observations of clouds in Titan's atmosphere (e.g. Griffith et al. 2005, Schaller et al. 2006 and Burratti et al. 2007), combined with work by Burr et al. (2006) and Collins (2005) suggesting that sediment transport rates (Burr et al.) and rates of fluvial erosion into bedrock (Collins) are within a factor of a few of terrestrial rates for these quantities, portray a positive picture for formation of incised channels on Titan.

Many researchers have utilized these results in subsequent papers. Perron *et al.* (2006) determined a drainage basin area for the Huygens network and applied empirical relationships between drainage basin area and precipitation needed to form channels. They concluded that precipitation-driven incision was the likeliest method of formation for this network, and that the precipitation rates they derived to form these features, 0.5-15 mm hr⁻¹, are consistent with atmospheric methane abundance. Soderblom *et al.* (2007a) considered other channels present in the Huygens images, concluding that some of these features seem to be more consistent with sapping features, or channels that are tectonically controlled. Barnes *et al.* (2007c) combined RADAR and VIMS to address composition of the channel bedrock and sediments, determining a connection between channels and their dark blue spectral unit. Lorenz et al. (2008a, in press) provided a thorough summary of channels seen so far in SAR images; their work is similar in some respects to this work, but we include quantitative analysis for channel lengths and stream order.

In this paper, we discuss fluvial features present in SAR data on Titan as an ensemble by first discussing the data and our process for measuring features, and then describing the features in the context of the terrain they dissect. We report the length and global distribution of the features that we observe, and discuss some implications of the size and distribution of channels on Titan.

CHAPTER 2

DATASET AND MEASUREMENTS

2.1 Cassini RADAR

The Cassini Titan Radar Mapper operates in four modes—altimetry, radiometry, scatterometry and synthetic aperture—at a wavelength of 2.17 cm (Elachi *et al.* 2004). In this work we focus only on the highest-resolution of these modes, the synthetic aperture radar (SAR) mode. The SAR mode of RADAR is active during fly-bys of altitude under 4000 km and returns images that are hundreds of kilometers wide and thousands long. Spatial resolution ranges from 300 m pixel⁻¹ at the center of the highest-resolution strips to something closer to 1.5 km pixel⁻¹ at either end (e.g. Elachi *et al.* 2005).

The images are returned as backscattered intensity, because the SAR instrument is self-illuminating. Thus surfaces that are rough on scales of a few centimeters will appear brighter than smoother surfaces, which reflect more signal in a specular manner, away from the instrument. It is an oversimplification to attribute the signal intensity only to surface roughness, since there are a number of factors that determine the backscatter intensity, among which is scattering from below the surface (sometimes called volume scattering). However, we make the tacit assumption that channels bright in comparison to the surrounding terrain are generally rougher, with the converse being true for radar-dark channels. In general, the precise value of the backscatter intensity is unimportant, as we study only morphology.

2.2 The SAR images

At the time this research was conducted, there were 15 Titan flybys with SAR data, and we analyzed the sets that were publicly accessible: Ta, T3, T7, T8, T13, T16, T17, T18 and T19. Of these, seven show curvilinear features that we interpret as possible fluvial channels. For these, we measured the extents in latitude and longitude of all of the channels to determine channel length. The data used were Basic Image Data Records (BIDRs); that is, gridded maps of the SAR data, normalized and corrected for incidence angle effects (Stiles 2005).

As we looked for roughly linear features in low-resolution we tried to identify only the most well resolved channels. Typically only the largest fluvial features may be identified with confidence. Where features seemed clearly related, we made limited extrapolations, mostly in the channel networks, to connect definite channel segments. Note that at the ~1km resolution of the SAR data, the designation “channel” refers to the entire river valley, not the actual beds through which fluid might flow. While we might be able to detect the very widest riverbeds, we make no claims to have found ‘rivers,’ only channel-like valleys.

2.3 Channel measurements

To measure the lengths of the channels, we registered the highest resolution images with latitude and longitude backplanes at the same resolution and traced the

channels out in short (<10 km) segments, recording the great circle distance between each point. We left the images in the oblique cylindrical coordinates used when each SAR swath was obtained (Stiles 2005). This coordinate system has an effective equator that follows the ground track of the spacecraft through the center of the strip, and since deviation from Cartesian distance for cylindrical coordinate systems is a factor of the cosine of latitude, great circle distance is well approximated over the short lengths we measured. SAR strips are generally no wider than 15° , which results in an error of less than 1% of the measured length for segments measured at the edges of a strip. We also note here that, while the actual resolution of the data may be on the order of 1 km pixel^{-1} , the highest-resolution image products available from the Cassini RADAR team are mapped to a constant 175 m pixel^{-1} grid, making it possible to measure a feature in segments that are quite short. Doing so is dangerous, however, as this extra resolution is artificial. The shortest segments we measured were all close to 1 km.

Measurements of channel widths and depths are required to estimate the volume of the streams on Titan. Where the channel boundaries are easily determined and the channel itself is wider than the resolution of the instrument, we again use great circle approximation to measure the width of the features. However, as noted by Barnes *et al.* (2007c), the exact boundaries of the feature are not always easily determined. Furthermore, the channel widths are often near or below the resolution limit, making any measurement of them dependent on the artificial enhancement of the image resolution. We are therefore unable to determine a width for any channel narrower than 350 m.

Altimetry data to provide topography for Titan is scarce, given that mode's limited spatial coverage (Gim *et al.* 2007). Therefore, most measurements of a feature's height, or in the case of channels, depth, must be derived from some property of the radar backscatter. One such method is radarclinometry, a process analogous to photoclinometry that assumes that all differences in backscatter are due to topography (e.g. Widley 1986). Elachi *et al.* (2006) conducted radarclinometric modeling that suggested a channel depth of approximately 200 m for small channels present in the T3 swath, while Lorenz (2008a) found that the T7 swaths indicated appreciable incision of several hundred meters.

CHAPTER 3

CHANNEL DESCRIPTION

In the results discussed below, we have identified a few general morphologies for the channels on Titan: stream networks similar to river systems seen on Earth, channels that seem associated with another surface feature, including the channels near the north polar lakes, and some unassociated with any larger structure.

3.1 Channel networks

Three SAR swaths show channels that seem to exhibit a branching pattern more typical of a rainfall-induced channel network (Figure 3.1). The first SAR swath to examine the southern latitudes of Titan, T7, displays several interconnected streams that extend southward for hundreds of kilometers (342 E – 347 E, 50 S – 58 S). The near-equatorial, bright region called Xanadu, which was imaged in T13, is dissected by dozens of stream segments connected in the largest of these networks, located between 210 E to 235 E in longitude and extending beyond the width of the strip (6 S to 14 S) in latitude. A second, smaller network flows roughly southward at the eastern edge of Xanadu (285 E – 289 E, 8 S – 13 S). Finally, a small channel network in the northern mid-latitudes, located in the southeastern end of the T19 strip, extends northeast (32 E – 41 E, 5 N – 10 N) out of the strip. Given the relatively coarse resolution, we do not believe we are seeing the smallest branches present in these networks.

FIGURE 3.1 Channel Networks

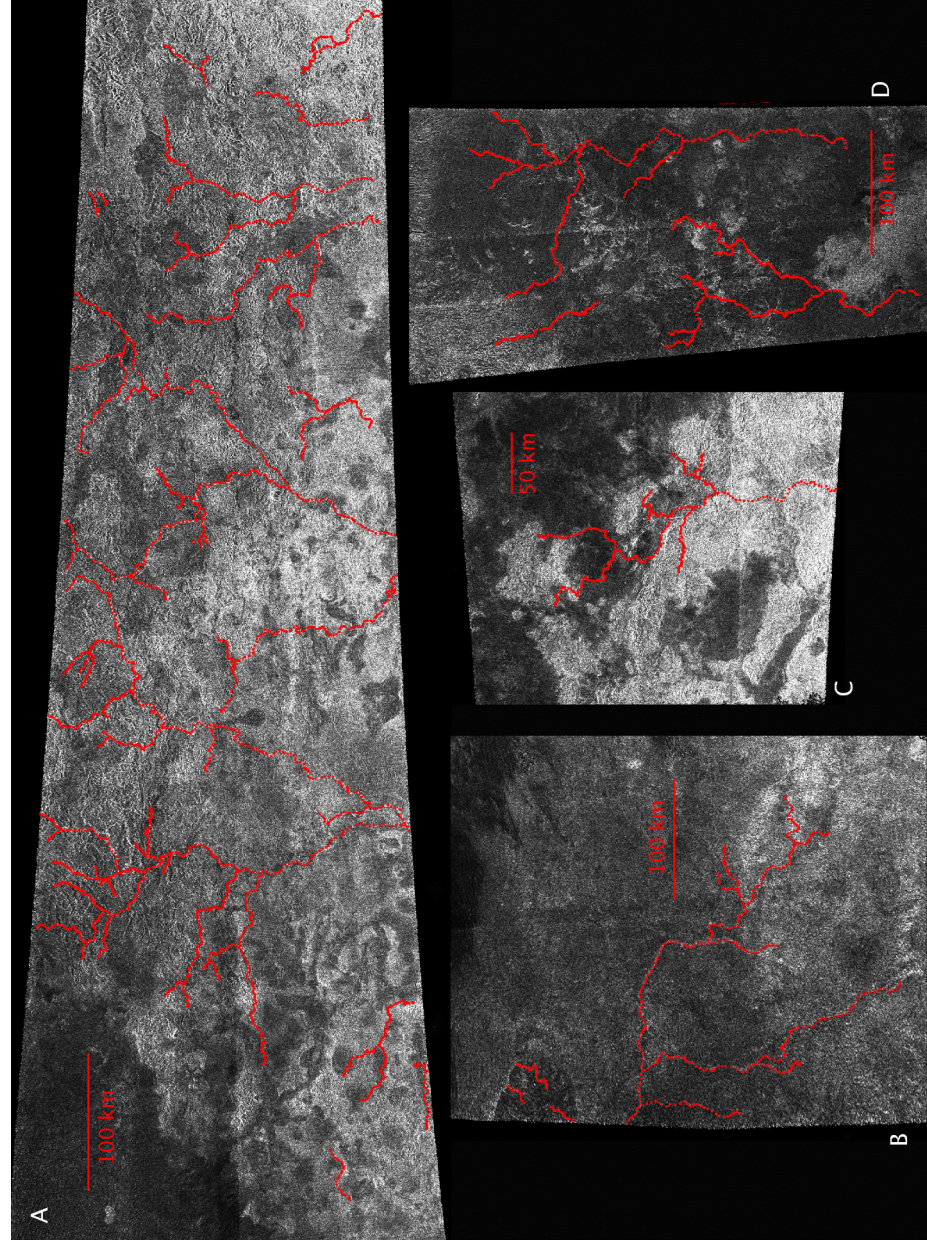


FIGURE 3.1: Four channel networks in SAR data on. In this and all subsequent images, latitude increases along the vertical, and positive east longitude increases along the horizontal. (A) T13 western network (B) T19 network (C) T13 eastern network (D) T7 network

The two networks from T13 are generally radar-bright, and are located at both the eastern and the western edges of the also radar-bright Xanadu. The eastern T13 network was particularly difficult to follow due to the range in signal of the terrain through which it flows, almost certainly disguising some tributaries that should have been resolved. The channels from T19 are cut into relatively featureless terrain, and the southern hemisphere T7 features appear in generally low-signal areas of the images in light/dark pairings indicative of incision (Elachi *et al.* 2006)

To the extent that it is possible to discern global correlation within the limited portion of the surface that RADAR has observed, there may be a preference for near-equatorial latitudes for these networks, although channels have been seen at all latitudes. There also seems to be a trend for flow away from the equator and towards the poles, an interpretation we discuss in further detail below (§4.2). Furthermore, it seems likely that this kind of channel network is relatively rare on the surface of Titan. Making a rough estimate of the surface area occupied by these three networks, and comparing that figure to the fraction of the surface so far imaged by RADAR, we see that only $\sim 3\%$ of the so-far viewed surface is occupied by channel networks. This is in stark contrast to Earth, where close to 100% of the land area has been modified by fluvial erosion (e.g. Baker 1986).

3.2 Channels associated with surface features

Some of the channels visible in the SAR swaths are juxtaposed with other visible features on the surface. This proximity may be coincidental, or the channels may have formed in response to either the event that formed the surface feature or to the topography these features impose upon the landscape. We discuss all channels located in close proximity to a surface feature in this section regardless of whether we think it is likely that the feature is the direct cause of the channels.

Ganesa Macula, first tentatively identified as a cryovolcanic feature by Elachi *et al.* (2005), is cut by at least three channels that either converge at or diverge from the center of the feature. Other channels to the east of Ganesa Macula have previously been identified as associated with the feature, possibly as a cryovolcanic flow field (Lopes *et al.* 2007).

If we were to consider only the branching of the channels on Ganesa Macula, which suggests that fluid has flowed from the rim to the center of the feature, we might conclude that the feature is perhaps a depression, rather than a dome as proposed by Lopes *et al.* (2007). Examining the branching patterns present to the east of the feature, direction of flow suggests a ridge near 51.0 N, 279.1 E (Figure 3.2), again in conflict with the results of Lopes *et al.* (2007), who note that flow directions are consistently to the southeast. We find radar-bright channels with branches in the east that seem to converge as they flow westward, terminating in smaller features (Figure 3.2 b) that bear some similarity to the fan-like structures identified by Lopes *et al.* (2007). This does not rule

FIGURE 3.2: Channels Near Ganesa Macula

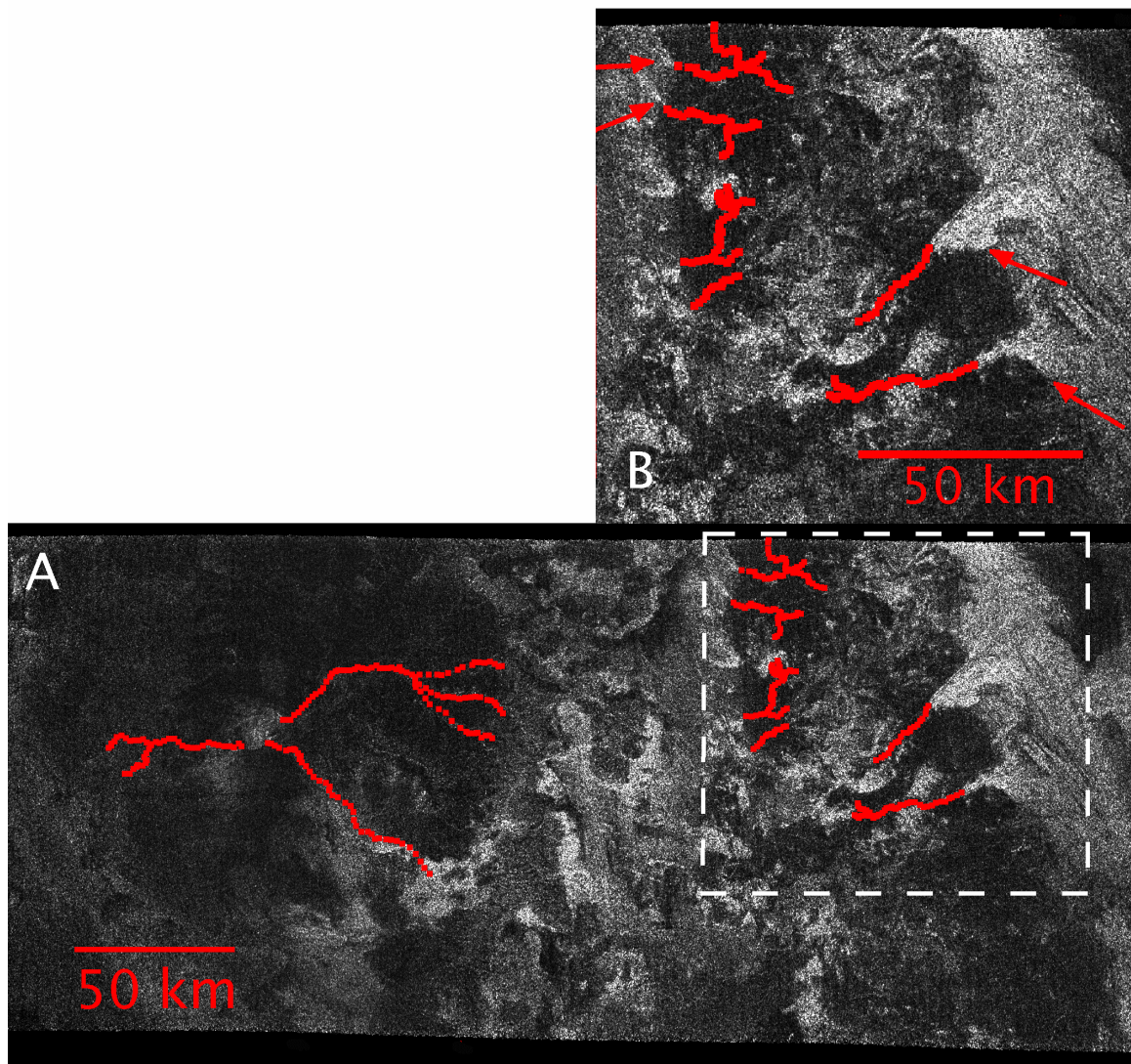


FIGURE 3.2:

(A) Ta near Ganesa Macula with traced channels. Note the channels to the right of the swath that seem to flow in opposite directions from a possible ridge.

(B) Inset of dashed region showing fanlike features at the termini of both eastward and westward flowing channels (marked by arrows).

out the interpretation of the mottled terrain as a lava flow field, but it does show that the data support other interpretations. Furthermore, there are some features in this field that Lopes *et al.* (2007) have identified as flow features that we do not outline, as we are looking for fluvial channels that appear to have been formed by precipitation rather than by cryovolcanism.

Similar to the fluvial channels near Ganesa Macula, some channels seem to be related to the large crater Menrva, seen in the T3 pass. Although it is difficult to draw detailed conclusions regarding the topographic features of the crater rim given resolution constraints, it does appear to be significantly degraded. Large channels are present on both sides of the southwestern rim, and the rugged nature of the northeastern rim, similar in appearance to crater rims seen in Mariner 9 images (Pieri 1976), suggests the presence of many shorter channels. The largest assemblage of the long channels is to the southwest of Menrva and appears to flow northeast into the crater, rather than down the exterior side of the rim (Figure 3.3). This runs counter to expectations of flow direction around a normally elevated feature such as a crater rim and further supports the idea that the rim, particularly the western edge, has been extensively weathered.

The other concentration of channels is located to the west of the crater. These channels display a unique morphology—channel width varies irregularly over the lengths of the channels and the direction of flow is unclear. Elachi *et al.* (2006) interpret these as a series of both braided and sinuous fluvial channels flowing northeastward away from the crater and draining into the large radar-bright region further east. Lorenz *et al.*

(2008a) concur with this interpretation, citing the similarity between this image and dry washes on Earth as support for the idea of anabranching channels.

3.3 Other channels on Titan

Most of the rest of the channels present on Titan seem clearly associated with lakes at high northern latitudes. Channels flow into and between many of the lakes currently thought to contain liquids, and there seems to be no preferred direction of flow or regional gradient near the lake region. These channels tend to be shorter than many of the features present in other Titanian stream networks, with a median length of about 15 km. There may also be channels near the features interpreted as dry lakebeds, but distinguishing these features from the dry lakebeds is difficult.

Other, generally short, channels are present elsewhere throughout the SAR images, mostly in mottled terrain where radar-bright, curvilinear features are common and can confuse the eye. Many apparent features also exist in the images. An example of a radar-dark region that might be a channel is seen (Figure 3.4) near the crater Ksa but, as stated before, we only consider a channel if we are confident that a feature truly exists.

FIGURE 3.3: Channels Near Menrva Crater

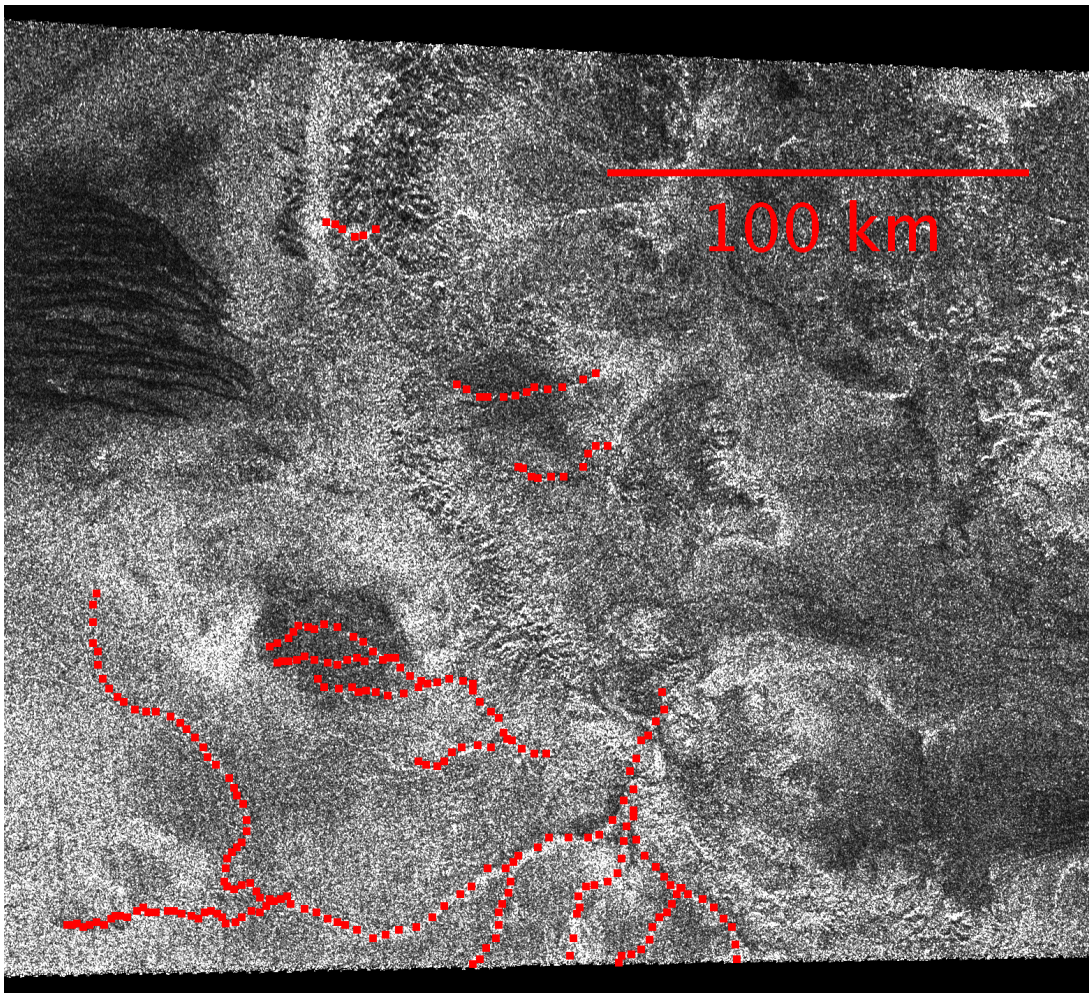


FIGURE 3.3: Note the branching channels that seem to flow northeast into Menrva Crater

FIGURE 3.4: Possible Channel Near Ksa Crater

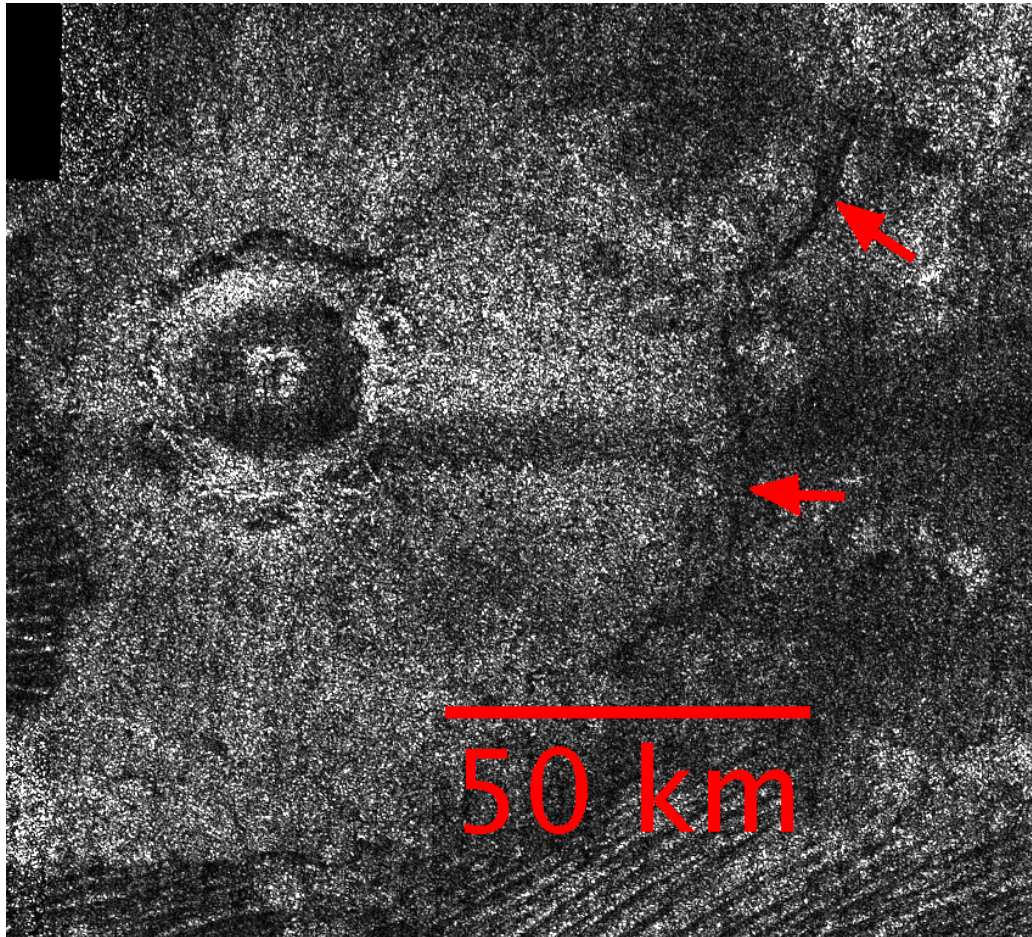


FIGURE 3.4: Ksa crater, with possible dark channel marked by the red arrows. Many similar features exist in the SAR images, but because we are not convinced that these represent fluvial features, we do not include them in our measurements.

CHAPTER 4 RESULTS AND DISCUSSION

4.1 Channel lengths

Determining the length of a channel can be approached in several ways. For several reasons we chose to measure actual distance traversed by a feature, rather than direct distance from headwaters to outflow. First, we use the actual distance traveled by flowing liquids in several calculations. Second, the source regions and outflow are often either off the edges of the RADAR swaths or otherwise difficult to locate. Finally, the relatively low resolution of the data makes determining the course of a river something of an art. We acknowledge that other researchers may trace slightly different channels than we have, and we therefore report the measurements of the actual channels we distinguished rather than requiring another layer of interpretation by the reader. Furthermore, even when several features are clearly interconnected, and where on Earth the reported length would be that of the main river segment, we still report total length of all channels, since it is not yet clear what the main channel of a feature would be. Appendix A contains the lengths of all channels we measured.

The manner in which we report channel lengths depends somewhat on the morphology of the channel. For most of the channels we considered the length of a segment to be from its start to where it either intersected another channel or ceased to be distinguishable from the background. Table 4.1 summarizes our results for the 237

channels we identified on the surface. The median length of all channels on Titan is 29 km. The shortest channels were not quite 3 km long and were between lakes; the longest, almost 350 km long, belonged to the southern channel network.

In addition, where a network was present, we counted stream order for the member channels. Stream order is a method of organizing tributaries of a river by size—first-order streams are the smallest branches of the network. Using Strahler’s (Strahler 1958) method of ordering, where two first-order streams intersect, they form a second order stream. Two intersecting second-order streams form a third-order stream, and so forth. A stream of lower order intersecting a stream of higher order does not affect the order of the larger stream—that is, the stream formed at the intersection of first- and second-order streams is second order. The ability of stream order to reveal information about channel formation mechanism or properties of the underlying rock has been largely dismissed, but where a true channel network is present, it is a convenient method of organizing results. We therefore present Strahler stream ordering for the features present on Xanadu, the southern end of the T7 swath and the southeastern end of the T19 swath in Table 4.2. Note that these channels are also included in the summary information in Table 4.1.

TABLE 4.1: Length of Streams on Titan

Length	Number
< 5 km	9
5 km-10 km	28
10 km-50 km	129
50 km-100 km	43
> 100 km	28

TABLE 4.2: Stream Order and Channel Lengths for Titan's Channel Networks

	Order	Number	Average Length (km)	Branching Ratio
T7	1	10	64	3.33
	2	3	203	3
	3	1	108 ^a	—
T13a	1	57	38	3
	2	19	98	4.75
	3	4	251	4
	4	1	16 ^a	—
T13b	1	7	50	2.33
	2	3	41	3
	3	1	165 ^a	—
T19	1	8	66	2.67
	2	3	69	3
	3	1	263 ^a	—

^aOnly channel of given order in network

The above statistics make good sense for fluvial features—higher order streams are in general longer (note that the fourth order stream present in T13 flows out of the edge of the strip), and the branching ratios are consistent with those seen on Earth. The highest order recorded for any channel on Titan so far is fourth order, but since properly determining order depends critically on resolving the small tributaries of a system, this result is not comparable to stream order of fluvial networks on Earth or Mars. It is certainly an underestimate. The stream network seen in the Huygens descent images also contains a 4th order stream (Soderblom *et al.* 2007b), and that network is not resolved in the corresponding SAR swath.

4.2 Geographic distribution of the channels

Any discussion of geographic correlations of the channels seen on Titan is of course subject to observational bias. At present, only the north polar region of Titan has been well covered by Cassini RADAR, with very limited coverage in the southern hemisphere and near the equator. Nevertheless, within existing coverage, a few telling features may be seen.

First, high-drainage-density stream systems, at least those large enough to be resolved by SAR, seem to be relatively rare on Titan. Furthermore, while streams appear in many of the radar images on Titan, they are not ubiquitous on the surface, again within the constraints of the spacecraft resolution. While it is possible that the Titanian landscape has experienced fluvial erosion as extensively as has Earth (where fluvial

features dominate the landscapes of even very arid regions) this modification must occur on scales below the resolution limit of RADAR. Furthermore, the preponderance of large channels is in the mid-latitudes, rather than near the polar regions as proposed by Porco *et al.* (2005). Here we must be especially careful, given that the south-polar region has not been well imaged. Nevertheless, the channels seen in the northern regions seem to be clearly associated with the lakes and are in general shorter and, except where they appear to empty into the lakes, narrower than the largest features in the Xanadu networks.

Second, as stated above, the direction of flow in the four channel networks, including three networks with apparent source regions within 10° of the equator, is away from the equator and toward the poles. This could indicate a general pole-ward transfer of fluid and sediment on the surface. Again we must emphasize the fact that large areas of Titan have yet to be observed by SAR, and thus this interpretation may be invalidated by later observations. Furthermore, the presence of large dune fields in the equatorial regions seems to argue for relatively low topography in that region, which could contradict our interpretation of channel flow direction. All of the surface liquid seen so far is also located at the poles (Stofan *et al.* 2007), and while methane drizzle has been observed at mid-latitudes (Ádámkovics *et al.* 2007), most of the large clouds thus far observed have been at latitudes higher than 40° (e.g. Griffith *et al.* 2005, Schaller *et al.* 2006, Buratti *et al.* 2007). These factors seem to suggest that the equatorial region is currently dry, making the idea of poleward transfer of fluid and sediment problematic. That being said, fluid must flow from higher terrain to lower terrain. It is possible that the downslope

direction as indicated by branching patterns in the network may only apply to the terrain immediately surrounding the channels, or, as there is no indication that fluid currently flows through these features, the channels may be relics and thus the indicated gradient may no longer exist. It is also possible that during a previous epoch on Titan, precipitation at lower latitudes was more common. However, if this trend does accurately reflect the current global shape of Titan, one possible explanation for the topography may have important implications for Titan's interior structure. In their 2007 paper on the shape of the Saturnian satellites, Thomas *et al.* demonstrated that the triaxial shape of Iapetus is inconsistent with its current rotational state. They report a fossil rotational bulge of over 30 km, substantially greater than the 10 km bulge predicted from satellite density and spin rate, and note that this is indicative of the shape of the satellite freezing at a spin rate of approximately 16 hours, rather than its current synchronous rotation, with very little subsequent deformation. If a similar fossil oblateness were to explain the direction of channel flow on Titan, the implied lack of relaxation from a fossilized rotational bulge to a shape in equilibrium with the current rotational state would make a subsurface ocean unlikely. A shape model for Titan based on observations of the limb of the planet does not currently exist, however, given the difficulty of observing that body's limb through its atmosphere, so at this point, such an explanation is still hypothetical.

Third, most of the channels seen on the surface seem to be associated with some outstanding topographical feature. This trend is not universal; for instance, the channel networks on T7 and T19 do not seem to be a part of some larger underlying structure, and

there are no large channels present near Sinlap or Ksa, but many channels are present in suspiciously close association with Menrva and Ganesa Macula, and the largest collection of channels on Titan cuts through Xanadu, which, while possibly not the ancient continent as originally proposed, (Momány *et al.* 2005) is certainly still a large, highly visible surface feature. These associations may be indicative of topographic influence on rainfall, as suggested by Lorenz (2006), or it may be simple coincidence. If the interpretation of a cryovolcanic origin for Ganesa Macula proves correct, however, this may strengthen the case for the fluvial features near that object representing volcanic outflow features, rather than precipitation-cut channels.

Finally, while the terrain on which we have identified channels varies widely, we do not see evidence of large channels flowing towards dune fields. One possible exception to this trend is the channel network on T19, which is just slightly south of a small patch of dunes.

4.3 Sediment budget on Titan

The extensive dune fields on Titan are believed to represent a massive volume of sand-sized particles (Lorenz *et al.* 2008). The composition of these dunes is an ongoing question in Titan research (e.g. Soderblom *et al.* 2007a), but because rivers on Earth are efficient systems for sand production and transport, the presence of fluvial features, and thus fluvial erosion, suggests a possible source for the sand. To test this hypothesis, we

calculated the order-of-magnitude volume of the channels on Titan as a rough estimate of the amount of sediment produced and transported by fluvial erosion.

The total length of the channels measured in this work is 1.21×10^7 m—a measurement that is fairly straightforward to obtain, but valley width and depth are more difficult to measure. As discussed previously, determining channel boundaries is challenging, especially where the features are either particularly narrow, found in the characteristic dark/bright pairing that indicates incision, or not sharply distinct from the background of the image. Reported widths vary between the resolution limit of the SAR instrument (itself a rather fuzzy quantity but certainly no finer than 300 m pixel^{-1}) to 7 km for the wide, possibly braided channels to the east of Menrva crater (Elachi *et al.* 2006). Barnes *et al.* (2007) have determined approximate channel widths of 800 m-2000 m based on spectral mixing ratios from VIMS data for some of the largest channels visible in those images. Most of the channels we discuss in this work are closer to the narrow end of these ranges, near 1-1.5 km. For channel depth we use the results of Lorenz (2008) and Elachi *et al.* (2006), who agree that incised channels have depths of 100-300 m.

Using a constant channel depth of 100 m and width of 1 km, we calculate total channel volume to be 10^{12} m^3 . We then extrapolate this volume to the global volume of stream-transported sediment by assuming that each radar strip reveals 1.5% of Titan's surface and that stream density on the entire body is similar to that on the SAR strips already seen, a process that gives us a lower limit of 10^{13} m^3 of sediment. If we compare this figure to the surface area of sediment represented by the VIMS (Barnes *et al.* 2007a)

dark brown spectral regions thought to be dominated by dunes (Barnes *et al.* 2007a, Soderblom *et al.* 2007a), and again assume that the dunes stand out above the resolution of the instrument (which is to say that they are approximately 100 m high), we calculate 10^{14} m^3 of dune sediment. This calculation agrees with an estimate of the same quantity by Lorenz *et al.* (2008b), who determine the volume of sediment represented by Titan's dune fields to be $2\text{-}8 \times 10^{14} \text{ m}^3$. We note that while this figure is in good agreement with our result, an additional work (Lorenz *et al.* 2008a) calculates that only approximately 0.1% of Titan's surface area is occupied by streams. Given our measured total length of 10^7 m , our assumed channel width of 1 km and our extrapolation from nine SAR swaths to all of Titan, we calculate that close to one percent of Titan's surface is covered by channels. This discrepancy may result from the fact Lorenz *et al.* (2008a) do not measure total channel length directly but estimate surface area coverage based on the length of the portions of SAR swaths that display obvious channels.

The above estimates do not account for the fact that streams certainly transport a much larger volume of sediment than that actually carved out of the underlying bedrock, so our number is likely an underestimate. Further, streams on Earth frequently take advantage of pre-existing tectonic features, a subtlety that our calculation fails to consider. The extrapolation from seven SAR swaths to the entire surface of Titan may also be inappropriate if precipitation is not isotropic. Our estimate of the volume of sediment present in the dune-filled regions is equally first-order, but the general agreement of these figures to a couple orders of magnitude indicates that, from a purely

volumetric argument, the dune particles could be explained as the products of stream erosion. This is in contrast to Lorenz *et al.* (2008a, 2008b), who state that fluvial erosion by the SAR channels is insufficient to explain the dune sediments. As noted above, our results differ from theirs by an order of magnitude.

The preceding explanation of the dune particles as fluvial sediment is likely incomplete for a couple of additional reasons. For example, the exact composition of the dunes is unknown (Soderblom *et al.* 2007a), but river sediments are likely to be representative of the substances into which the channels are carved. Titan's bulk density argues for a composition with a high fraction of water ice, including a water ice surface (Tobie *et al.* 2005), and evidence from ground-based observations (Griffith *et al.* 2003) and the VIMS instrument (Buratti *et al.* 2006) further support the presence of water ice on the surface. The few features that have been interpreted as depositional are all radar-bright (Elachi *et al.* 2006, Lopes *et al.* 2007). The dunes, on the other hand, are quite dark in RADAR and ISS (Porco *et al.* 2005) as well as VIMS spectral windows (Barnes *et al.* 2007b), and are relatively water-poor (Soderblom *et al.* 2007a), suggesting compositional differences between the channel bedrock and dune materials. Soderblom *et al.* (2007a) argue for a completely different composition, like an aggregate of atmospheric hydrocarbons, while Barnes *et al.* (2007b) state that the possibility of a hydrocarbon coating over water ice cannot be ruled out.

Furthermore, not all of the material removed and transported by streams will be reduced to sand-sized particles, thus introducing another unknown factor in this

comparison. However, the largest inconsistency with this theory is that at the resolution of the RADAR instrument there seems to be no correlation between dune-filled regions and depositional features at the termini of channels. This is in agreement with the idea that there seems to be a general transfer of fluid, and thus sediment, away from the equator and toward the poles. In contrast, most of the dune fields imaged so far are near Titan's equator. Again examining the extensive channel network seen on the western edge of Xanadu (Figure 4.1), we see channels on the boundary between the bright regions and darker dune-filled areas. These channels flow southeast, away from the dune-filled region rather than towards it. Recent work by Wood *et al.* (2007) shows evidence that Xanadu is a topographic low rather than an ancient continent as previously suggested. Our interpretation of channel flow in this region supports these results. We do note that at scales smaller than RADAR resolution this interpretation may be invalid, as demonstrated by the Huygens probe. That instrument landed on a depositional surface (as evidenced by the presence of sediment and cobbles, Tomasko *et al.* 2005) that was only a short distance away from many dunes.

FIGURE 4.1: Edge of the Western Xanadu Network

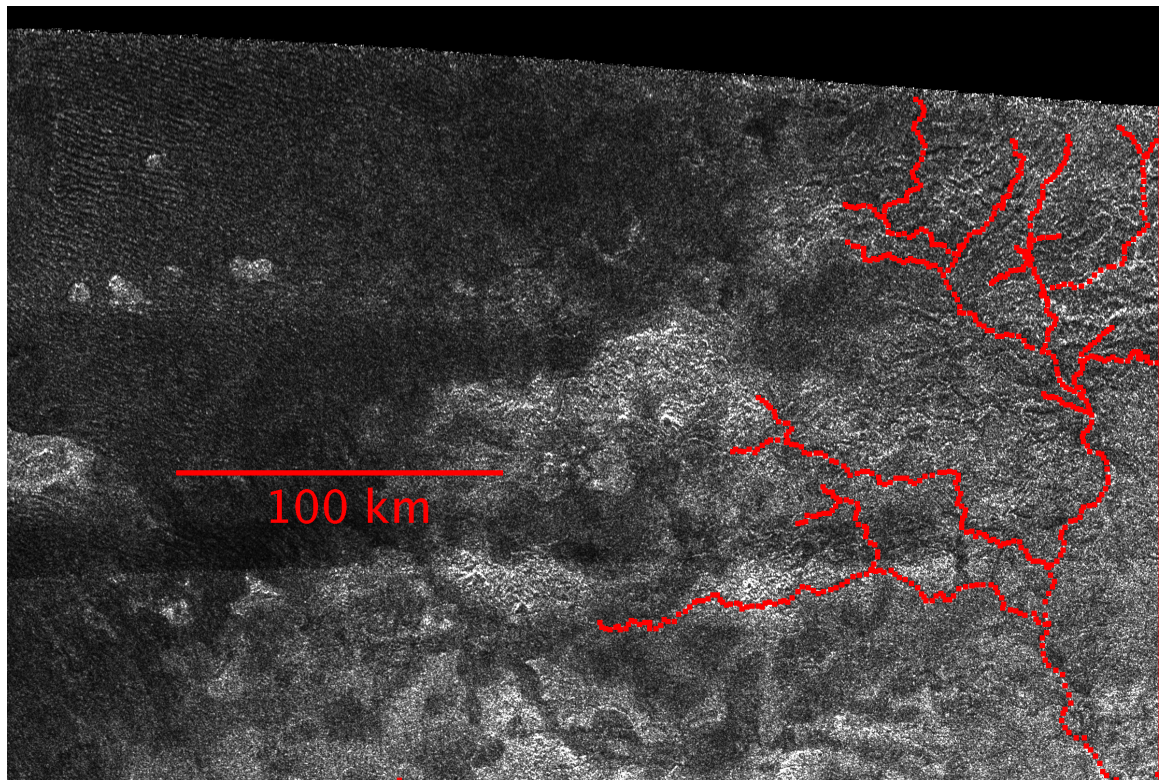


FIGURE 4.1: Western edge of Xanadu and the channel network. Note the dunes to the northwest and the southeast direction of flow in the channel network. Lack of any indication of flow from the edge of the bright regions into the darker, dune-filled region supports the notion of Xanadu as a low-lying region, instead of a local elevation.

4.4 Channel network integration

Because directly measuring the amount of sediment transport from the channels on Titan is difficult, another feature of these channels may suggest an alternate method. The channels present on Xanadu and those revealed in T7 seem to be well-established, almost fully integrated channel networks. Down to the resolution limit of the images, there are few unconnected drainage features, suggesting that these features are relatively old. Within the $\sim 3 \times 10^5 \text{ km}^2$ area encompassing all of the channels on Xanadu, 79% by length of the streams are integrated into one of the large order streams (Figure 4.2).

That a few of Titan's channels exhibit this level of organization may provide a tool for determining the amount of sediment those streams have transported. For what is initially a disorganized ensemble of small, disjointed streams to unite and form the kind of features seen on Titan, years of rainfall and sediment transport must occur. The exact time span is difficult to estimate, however, especially since it depends both on the rate of rainfall and on the overall gradient of the terrain. Stated another way, a large amount of sediment must be worn off of the highs of a landscape and transported to depressions for a stream to continue following an overall gradient, a process described by Glock (1931). While this process does take some time, the total volume of sediment that must move may be estimated independent of time using landscape evolution models that incorporate reasonable assumptions about initial topography.

FIGURE 4.2: Stream Order in the Western Xanadu Network

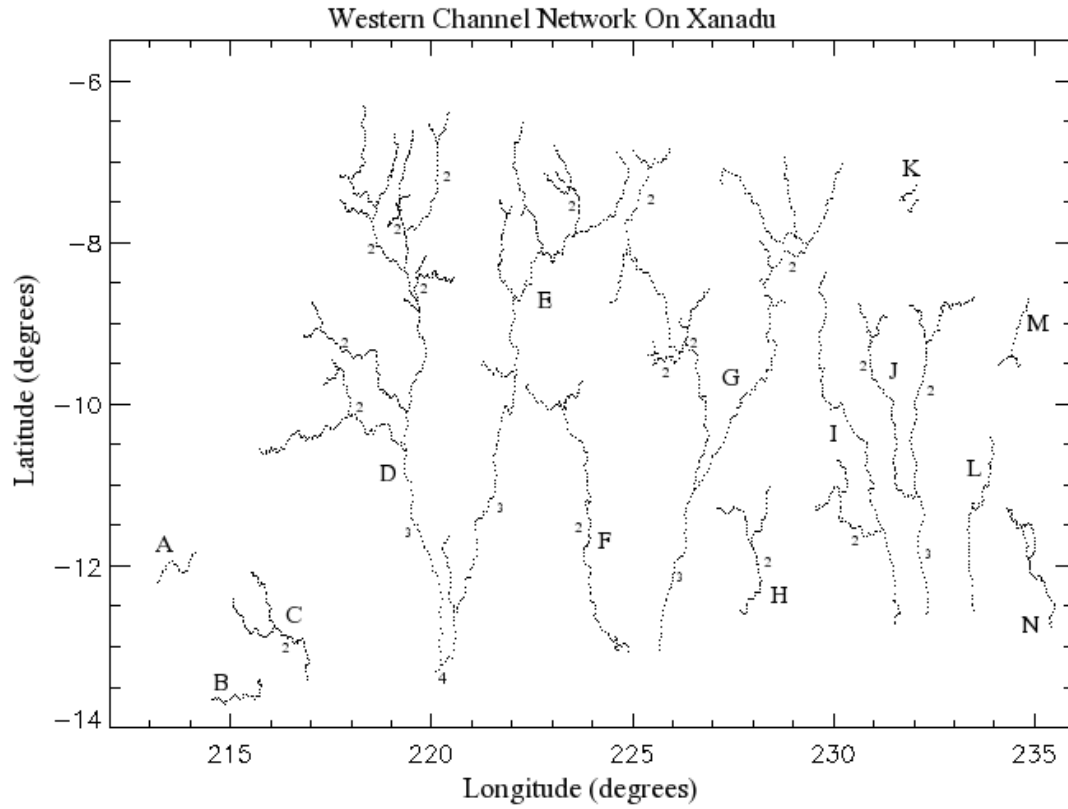


FIGURE 4.2: The western channel network from T13. Channels A-C, F, H and K-N are not incorporated into a high-order stream. Incorporated channels of second- or higher order are marked as such. All other unmarked incorporated channels are first-order.

CHAPTER 5

CONCLUSIONS AND FURTHER QUESTIONS

We measured 237 channels in SAR images of the surface of Titan. These channels had a median length of 29 km, with a minimum length of under 3 km and a maximum length of over 300 km. Within the limitations of the SAR coverage of Titan, most of these channels are located within 60° of the equator, with branches near the equator combining to form larger channels at larger latitudes, indicating that there may be net transport of fluid and sediments from lower to higher latitudes. Many of the features we interpret as fluvial seem directly related to topographic structures on the surface.

Roughly half of the large channels on Titan are organized into branching networks that qualitatively resemble river systems on Earth and Mars. Furthermore, the networks are large and well integrated, suggesting significant rainfall and fluvial erosion have occurred on the surface. Work by Burr *et al.* (2005) discusses the carrying capacity of liquid methane to transport water ice sediment. If modeling can constrain the amount of sediment that has been transferred by these networks, that result could be combined with Burr's results to extrapolate the volume of liquid methane needed to carry that load away.

The total length of the channels, combined with estimates of width and depth, yields a volume of sediment that is roughly consistent with the volume of sand contained in Titan's dune fields. Even so, a fluvial origin for this sand, while not ruled out by this

calculation, is unsatisfying based on the lack of association of channels with the dune fields and uncertain correlations between sediment and riverbed composition. This of course leaves the question of how the dune particles were produced and poses an additional problem: where are the alluvial deposits? Depositional features are not present in great abundance at the termini of channel features. Some features near Ganesa Macula have been interpreted as alluvial fans (Lopes 2007, this work), and Elachi *et al.* (2006) interpret the large bright region to the east of Menrva as a depositional feature.

Nevertheless, these cannot represent the only depositional structures on Titan, and if there is another sand sea's worth of loose sediment on Titan, where is it and how does it behave? Further research into the composition, behavior and formation mechanisms of the fluvial features on Titan will help to clarify these and other outstanding questions.

APPENDIX A

CHANNEL LENGTHS FOR ALL SAR SWATHS

SAR swath	Channel Length (km)	SAR swath	Channel Length (km)	SAR swath	Channel Length (km)
TA	3.5	T13	8.4	T13	24.5
	3.9		9.3		38.9
	4.4		10.0		52.7
	5.4		11.7		72.4
	5.9		13.3		127.4
	6.5		13.8	T16	5.6
	6.6		14.4		10.5
	7.1		15.9		11.7
	7.7		16.1		21.6
	7.9		17.3		21.6
	9.3		18.2	T18	29.9
	13.0		18.7		63.7
	14.0		18.8		3.1
	15.1		18.9		3.9
	15.6		20.7		3.9
	16.7		22.1		6.4
	16.7		22.9		6.8
	19.3		23.1		6.8
	19.4		24.0		7.4
	19.7		27.6		7.5
	20.0		28.2		12.2
	23.4		28.9		13.5
	26.0		31.5		15.0
	29.6		32.4		15.4
	31.2		32.5		15.6
	32.1		32.5		18.4
	32.9		32.9		20.6
	33.0		35.8		20.8
	34.9		35.9		21.5
	51.9		37.5		23.7
	52.4		43.7		30.2
	74.2		44.3		36.7
T3	13.7		44.6		45.5
	23.9		45.5		45.5
	24.3		46.1		46.4
	24.4		50.1		49.6
	26.9		50.3		63.4
				T19 (1 st order)	
	27.2		52.1		27.2
	28.6		52.2		35.3
	29.3		52.3		43.5

SAR swath	Channel Length (km)	SAR swath	Channel Length (km)	SAR swath	Channel Length (km)
	33.4		55.0		46.0
	36.6		56.4		58.0
	41.9		57.8		66.6
	51.3		57.8		91.1
	56.5		61.3		166.5
	57.6		61.7	2 nd order	17.9
	102.6		63.7		76.4
	106.7		76.0		114.0
T7 (1 st order)	23.5		94.2		263.8
	25.2		111.8	not incorporated	2.3
	35.6		119.0		4.6
	36.6		210.7		5.7
	36.8	2 nd order [†]	11.0		8.2
	49.6		15.1		8.3
	77.6		19.9		8.5
	82.8		33.8		9.8
	86.9		37.5		9.9
	185.8		57.8		10.9
2 nd order	102.9		61.0		11.2
	163.5		61.6		12.0
	343.9		62.8		13.1
3 rd order	108.6		76.0		13.6
not incorporated	107.9		91.5		14.2
T13 (1 st order)*	6.8		97.2		17.3
	23.6		116.2		18.6
	29.7		132.3		19.8
	37.3		133.1		21.4
	66.8		133.7		22.2
	86.8		157.2		23.3
	105.6		212.4		24.7
2 nd order*	18.6		262.5		25.1
	23.3	3 rd order [†]	169.1		25.3
	81.6		225.5		36.6
3 rd order*	165.1		291.4		41.3
1 st order [†]	4.6		318.5		41.6
	6.5	4 th order [†]	16.6		46.2
	6.5	not incorporated	13.1		49.8
	7.5		14.0		85.0
	7.8		15.6		90.0

*Western Xanadu network channels

[†]Eastern Xanadu network channels

REFERENCES

- Ádámkovics, M., Wong, M. H., Labor, C. and de Pater, I., 2007. Widespread Morning Drizzle on Titan. *Science* 318, 962-965.
- Baker, V.R., 1986. Fluvial Landforms. In: Short, N. M. and Blair, R. W. (eds) *Geomorphology from Space: A Global Overview of Regional Landforms*. NASA SP-486, pp. 255-315
- Barnes, J.W., Brown, R.H., Soderblom, L., Buratti, B.J., Sotin, C., Rodriguez, S., Le Mouèlic, S., Baines, K.H., Clark, R., Nicholson, P., 2007a. Global-scale spectral variations on Titan seen from Cassini/VIMS. *Icarus* 186, 242-258.
- Barnes, J. et al., 2007b. Photoclinometry, Morphometry, and Spectroscopy of Titan's Sand Dunes from Cassini/VIMS. In: AGU Fall Meeting 2007. Abstract P23B-1354.
- Barnes, J. *et al.*, 2007c. Near-Infrared Spectral Mapping of Titan's Mountains and Channels. *J. Geophys. Res.* 112, E11006.
- Buratti, B.J., Pitman, K.M., Baines, K., Sotin, C., Brown, R.H., Clark, R.N., Nicholson, P.D., Griffith, C.A., Le Mouèlic, S. Momary, T., 2007. A mid-latitude cloud eruption on Titan observed by the Cassini Infrared Mapping Spectrometer. In: AGU Fall Meeting 2007. Abstract P23B-1358.
- Buratti, B.J. *et al.*, 2006. Titan: Preliminary results on surface properties and photometry from VIMS observations of the early flybys. *Planet. Space Sci.* 54, 1498-1509.
- Burr, D.M., Emery, J.P., Lorenz, R.D., Collins, G.C., Carling, P.A., 2006. Sediment transport by liquid surficial flow: Application to Titan. *Icarus* 181, 235-242.
- Collins, G.C., 2005. Relative rates of fluvial bedrock incision on Titan and Earth. *Geophys. Res. Lett.* 32, L22202.
- Elachi, C. *et al.*, 2004. Radar: the Cassini Titan Radar Mapper. *Space Sci. Rev.* 115, 71-110.
- Elachi, C. *et al.*, 2005. Cassini Radar Views the Surface of Titan. *Science* 308, 970-974.
- Elachi, C. *et al.*, 2006. Titan Radar Mapper observations from Cassini's T3 fly-by. *Nature* 441, 709-713.

Gim, Y., Stiles, B., Callahan, P. S., Johnson, W. T., Hensley, S., Hamilton, G., West, R., Alberti, G., Flamini, E., Lorenz, R. D., Zebker, H. A., Cassini RADAR Team, 2007. Titan Topography: A Comparison Between Cassini Altimeter and SAR Imaging from Two Titan Flybys. In: AGU Fall Meeting, Abstract P23B-1351.

Glock, W.S., 1931, The Development of Drainage Systems: A Synoptic View. *Geograph. Rev.* 21, 475-482.

Griffith, C.A., Owen, T., Geballe, T.R., Rayner, J., Rannou, P., 2003. Evidence for the Exposure of Water Ice on Titan's Surface. *Science* 300, 628-630.

Griffith, C.A. *et al.*, 2005. The Evolution of Titan's Mid-Latitude Clouds. *Science* 310, 474-477.

Lopes, R.M.C. *et al.*, 2007. Cryovolcanic features on Titan's surface as revealed by the Cassini Titan Radar Mapper. *Icarus* 186, 395-412.

Lorenz, R.D. *et al.*, 2008a. Fluvial Channels on Titan : Initial Cassini RADAR Observations. *Icarus*, in press.

Lorenz, R.D. *et al.*, 2008b. Titan's inventory of organic surface materials. *Geophys. Res. Lett.* 35, L02206

Momary, T. W., Baines, K.H., Buratti, B.J., Cassini VIMS Team, 2005. Elevated Features on Titan: Both Topographic and Atmospheric. *Bull. Am. Astron. Soc.* 37 (2005) Abstract 46.10.

Perron, J.T., Lamb, M.P., Koven, C.D., Fung, I.Y., Yager, E. and Ádámkovics, M., 2006. Valley formation and methane precipitation rates on Titan. *J. Geophys. Res.* 111, E1001.

Pieri, D., 1976. Distribution of Small Channels on the Martian Surface. *Icarus* 27, 25-50.

Porco, C. *et al.*, 2005. Imaging of Titan from the Cassini spacecraft. *Nature* 434, 159-168

Schaller, E.L., Brown, M.E., Roe, H.G., Bouchez, A.H., Trujillo, C.A., 2006. Dissipation of Titan's south polar clouds. *Icarus* 184, 517-523.

Soderblom, L. *et al.*, 2007a. Correlations between Cassini VIMS spectra and RADAR SAR images: Implications for Titan's surface composition and the character of the Huygens Probe Landing Site, *Planet. Space Sci.* 55, 2025-2036

Soderblom, L.A. *et al.*, 2007b. Topography and geomorphology of the Huygens landing site on Titan. *Planet. Space Sci.* 55, 2015-2024.

Stiles, B., 2005. Cassini Radar Basic Image Data Records SIS, JPL D-27889, version 1.4

Stofan, E. *et al.*, 2007. The lakes of Titan. *Nature* 445, 29-30

Strahler, A. N., 1958. Dimensional analysis applied to fluvially eroded landforms. *Bull. Geol. Soc. Am.* 69:3, 279-300

Thomas, P.C. *et al.*, 2007. Shapes of the Saturnian icy satellites and their significance. *Icarus* 190, 573-584.

Tobie, G., Grasset, O., Lunine, J. I., Mocquet, A., Sotin, C., 2005. Titan's internal structure inferred from a coupled thermal-orbital model. *Icarus* 175, 496-502

Tomasko, M. G. *et al.*, 2005. Rain, winds and haze during the Huygens probe's descent to Titan's surface. *Nature* 438, 765-778

Wilkey, R.L. 1986, Radarclinometry for the Venus radar mapper. *Photogramm. Eng. Remote Sensing* 52, 41-50.

Wood, C., Kirk, R. L., Stofan, E., Stiles, B., Zebker, H., Ostro, S., Radebaugh, J., Lorenz, R. D., Callahan, P., Wall, S., 2007. Xanadu is Old, Rugged and Low-lying. *DPS Meeting Abstract* 39, 44.05